Alzheimer's Disease Amyloid Propagation by a Template-Dependent Dock-Lock Mechanism†

William P. Esler,[‡,§] Evelyn R. Stimson,[‡,§] Joan M. Jennings,[§,||] Harry V. Vinters,[⊥] Joseph R. Ghilardi,[#] Jonathan P. Lee,[▽] Patrick W. Mantyh,[#] and John E. Maggio*[,‡]

Department of Pharmacology & Cell Biophysics, University of Cincinnati College of Medicine, Cincinnati, Ohio 45267, Department of Biological Chemistry & Molecular Pharmacology, Harvard Medical School, Boston, Massachusetts 02115, Department of Preventative Sciences, University of Minnesota, Minneapolis, Minnesota 55455, Department of Pathology & Laboratory Medicine and Brain Research Institute, University of California—Los Angeles Medical Center, Los Angeles, California 90024, and Department of Chemistry, Boston University, Boston, Massachusetts 02115

Received December 22, 1999; Revised Manuscript Received March 7, 2000

ABSTRACT: Amyloid plaques composed of the peptide Aβ are an integral part of Alzheimer's disease (AD) pathogenesis. We have modeled the process of amyloid plaque growth by monitoring the deposition of soluble Aβ onto amyloid in AD brain tissue or synthetic amyloid fibrils and show that it is mediated by two distinct kinetic processes. In the first phase, "dock", Aβ addition to the amyloid template is fully reversible (dissociation $t_{1/2} \approx 10$ min), while in the second phase, "lock", the deposited peptide becomes irreversibly associated (dissociation $t_{1/2} \gg 1000$ min) with the template in a time-dependent manner. The most recently deposited peptide dissociates first while Aβ previously deposited becomes irreversibly "locked" onto the template. Thus, the transition from monomer to neurotoxic amyloid is mediated by interaction with the template, a mechanism that has also been proposed for the prion diseases. Interestingly, two Aβ peptides bearing primary sequence alterations implicated in heritable Aβ amyloidoses displayed faster lock-phase kinetics than wild-type Aβ. Inhibiting the initial weak docking interaction between depositing Aβ and the template is a viable therapeutic target to prevent the critical conformational transition in the conversion of A$\beta^{(\text{solution})}$ to A$\beta^{(\text{amyloid})}$ and thus prevent stable amyloid accumulation. While thermodynamics suggest that inhibiting amyloid assembly would be difficult, the present study illustrates that the protein misfolding diseases are kinetically vulnerable to intervention.

INTRODUCTION

While many human diseases are a consequence of defects encoded at the gene level, others appear to result from alterations in the conformation of endogenous and otherwise nonpathogenic proteins (*1*−*3*). Consequent abnormal assembly of endogenous proteins has been implicated as the proximal cause of well over a dozen human diseases. Although there is little primary sequence homology among the involved protein monomers, the ability of each to undergo a significant conformational alteration to produce stable insoluble β-sheet assemblies is of paramount importance to both the etiology and pathogenesis of the disease state (*1*−*3*).

An abundance of strong circumstantial evidence suggests that brain senile amyloid plaques, composed of fibrillar assemblies of the naturally occurring 39−43 amino acid peptide Aβ,[1] contribute directly to Alzheimer's disease (AD) pathogenesis (*4*, *5*). While formation of this amyloid is thermodynamically very favorable, transition from the partially folded solution conformation (*6*−*8*) [A$\beta^{(\text{solution})}$] to the β-sheet amyloid conformation (*9*−*11*) [A$\beta^{(\text{amyloid})}$] is kinetically limited (*2*, *10*−*14*). Thus in AD, as in other protein assembly disorders, understanding the kinetic nature of the transition from A$\beta^{(\text{solution})}$ to A$\beta^{(\text{transition state})}$ and to A$\beta^{(\text{amyloid})}$ may illuminate the molecular etiology of the disease.

The process of AD amyloid plaque growth can be modeled under near physiological conditions by monitoring the addition or deposition of physiological concentrations (pM to nM) of labeled monomeric Aβ onto preexisting amyloid fibrils in human AD cortex (*15*−*17*). In sharp contrast to the process of in vitro nascent amyloid formation (aggregation) (*18*, *19*), stable Aβ addition onto preexisting amyloid (deposition) follows linear time dependence and first-order kinetic dependence on soluble Aβ concentration (*17*, *19*, *20*). As in the prion diseases (*21*), a significant conformational transition is critical to Aβ assembly and alterations in the

† This work was supported by the National Institutes of Health (AG-12853, AG-12435, AG-16570, AG-13775, AG-11852).

* To whom correspondence should be addressed: Department of Pharmacology and Cell Biophysics, University of Cincinnati College of Medicine, PO Box 670575, Cincinnati, OH 45267-0575. Tel. 513-558-4723; Fax: 513-558-1169; email: John.Maggio@uc.edu

‡ University of Cincinnati.

§ These authors contributed equally to this work.

|| Harvard Medical School.

⊥ University of California, Los Angeles Medical Center.

University of Minnesota.

▽ Boston University.

[1] Abbreviations: Aβ, human β-amyloid peptide; A$\beta^{(\text{solution})}$, A$\beta^{(\text{transition state})}$, A$\beta^{(\text{amyloid})}$, A$\beta$ in the solution phase, the transition state between solution and amyloid phases, and the amyloid phase, respectively; AD, Alzheimer's disease; BSA, bovine serum albumin; Ci/mmol, Curies per millimole; CSF, cerebrospinal fluid; [^{125}I]Aβ, [^{125}I]iodotyrosine^{10}-human Aβ(1−40)-OH; MALDITOF-MS, matrix-assisted laser desorption time-of-flight mass spectroscopy; PBS, phosphate-buffered saline; RP-HPLC, reversed-phase high-performance liquid chromatography.

10.1021/bi992933h CCC: $19.00
Published on Web 05/04/2000

energy barrier to this transition may influence susceptibility to the disease (*2*, *12*, *14*). Further, the ability of soluble Aβ to adopt a partially folded metastable conformation appears critical for assembly of the peptide (*2*, *6*, *8*, *22*).

On the basis of these observations, we hypothesize that the conformation of A$\beta^{(solution)}$ is critical for interaction with the amyloid template prior to the conformational transition. In such a case, preassembled amyloid would help mediate conversion of A$\beta^{(solution)}$ to A$\beta^{(transition\ state)}$ and eventually to A$\beta^{(amyloid)}$ by providing a "template" to guide conformational rearrangement by an induced fit mechanism. The recent development of an immobilized synthetic Aβ amyloid template (*23*, *24*) has allowed us to examine early events in Aβ deposition that precede stable association. Here we illustrate that interaction with preexisting amyloid, and perhaps with other templates, facilitates conversion of A$\beta^{(solution)}$ to A$\beta^{(amyloid)}$.

EXPERIMENTAL PROCEDURES

Peptides and Radiotracers. Synthetic Aβ(1−40), Aβ(1−42). and Aβ(1−40)-E22Q (all >98% pure), lots 0313615, 0311202, and 0321302, respectively, were purchased from Quality Controlled Biochemicals (Hopkinton, MA). The peptides were characterized by reversed-phase HPLC (RP-HPLC), matrix-assisted laser desorption time-of-flight mass spectrometry (MALDITOF-MS), and amino acid analysis with satisfactory results in all cases. Peptides were stored desiccated at −20 °C.

Peptides were radioiodinated as previously described (*24*). Briefly, Aβ congeners were radiolabeled at tyrosine 10 by oxidative iodination using Na^{125}I and chloramine T. Peptide and unincorporated iodide were separated by reversed-phase adsorption. The oxidized methionine at position 35 was reduced from the sulfoxide to native thioether form using 2-mercaptoethanol. The radiolabeled Aβ congeners were purified by RP-HPLC to essentially quantitative specific activity and were stored at −20 °C in the eluted HPLC mobile phase. 2-Mercaptoethanol (0.5%) was added to all stock tracer solutions to prevent oxidation during storage. For double label experiments, [^{131}I]Aβ(1−40) was prepared using Na^{131}I and the same method described for ^{125}I-Aβ. The radiolabeled Aβ peptides produced by this method have been found to accurately track unlabeled Aβ in a wide range of experiments (*24*).

Aβ Deposition Experiments. Synthetic amyloid (synthaloid) templates were prepared by immobilizing highly ordered fibrils in 96 well plates as described (*23*, *24*). For deposition on-rate experiments, [^{125}I]Aβ(1−40) was diluted to a final concentration of 100 pM in PBS (10 mM NaH_2PO_4/Na_2HPO_4, 100 mM NaCl, pH 7.5) containing 0.1% BSA and incubated at room temperature with immobilized synthetic amyloid fibrils in the wells of 96-well plates as described. After the desired incubation, the radiolabeled Aβ solution was removed and the fibrils were washed (3 × 30 s with agitation) using an automated microplate washer. The amount of radiolabeled Aβ incorporated into the fibrils was then quantified by γ-counting. Control experiments were performed using fibrils prepared from reverse sequence Aβ, performed using peptide not deliberately aggregated, fibrils prepared from reverse sequence Aβ, or wells containing no aggregates; all these had negligible activity as templates. Experiments were performed with at least five replicate and three control wells at each time point.

For dissociation experiments, radiolabeled Aβ was loaded onto the fibrils as described above. After the desired load time, the remaining soluble radiolabeled Aβ was removed and the fibrils rapidly rinsed (less than 30 s). The wells were then soaked with buffer in the absence of free Aβ. To ensure that the concentration of free Aβ remained negligible, the soaking buffer was replaced frequently. At each time point, the wash buffer was removed and the quantity of the radiolabeled Aβ remaining bound to the template was quantified by γ-counting.

For dissociation (off-rate) experiments of Aβ deposited ex vivo onto brain amyloid, [^{125}I]Aβ was deposited onto slide mounted sections of unfixed cerebral cortex from an autopsy confirmed case of AD (*15*−*17*, *24*). After incubating with the tissue for 10 or 1050 min, the radiolabeled Aβ solution was removed and the tissue was briefly (5 s) rinsed with buffer. The sections were then soaked in buffer for 5, 30, 120, and 360 min to examine dissociation of the deposited Aβ. The sections were then imaged as dark-field autoradiograms, where light areas represent the sites and intensities of radiolabeled Aβ deposition. Different film exposure times were used for the short (10 min) and long (1050 min) load time experiments so the images would be of comparable intensity at the 5 min dissociation time.

For double label experiments, we utilized [^{125}I]Aβ and [^{131}I]Aβ, which can be unambiguously distinguished by γ-emission energies, to allow determination of the temporal sequence of dissociation for alterations in pulse and chase time length for exposure to a template of synthetic amyloid. Following a pulse of one radiolabeled Aβ isotope and a chase with the second radiolabeled Aβ isotope, dissociation times for the two isotopes were measured as described above. Results were indistinguishable whether ^{125}I and ^{131}I were used for isotope A and isotope B, respectively, or isotope B and isotope A, respectively.

RESULTS

To examine the mechanism of amyloid propagation, we measured the deposition of radiolabeled Aβ at physiologically relevant concentrations onto a template of immobilized synthetic Aβ fibrils. Consistent with previous results (*16*, *17*, *23*), the amount of Aβ deposited on the time scale of hours displayed linear time dependence. However, examining deposition on a much shorter time scale revealed more complex kinetics (Figure 1). Aβ deposited onto the template in two kinetically distinct phases, consistent with a multistep process with a rate-limiting step. At short times (less than 30 min) or long times (greater than 2 h), the Aβ deposition time course was linear (r^2 = 0.96 and 0.97, respectively), with the slope of the first linear phase substantially (about 8-fold) greater than the slope of the second linear phase.

To examine how these processes affected the stability of deposited Aβ, we determined dissociation rates of deposited Aβ for each of several load times spanning both linear phases and the intermediate portion of the deposition time course. In contrast to what would be expected for a simple dissociation process, load time had a dramatic effect on the fraction of Aβ that remained bound to the template over long dissociation times (Figure 2a). When Aβ was deposited onto

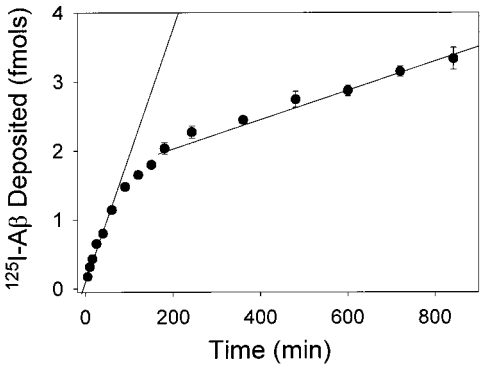

FIGURE 1: Time course of radiolabeled Aβ deposition onto immobilized amyloid fibrils. Error bars represent the standard deviation of five replicates. Error bars that are not visible are smaller than the symbols. The lines shown represent linear regression best fits of the first and second linear phases, $r^2 = 0.96$ and 0.97, respectively.

the template for a short time (within the first linear phase in Figure 1), nearly all of the deposited peptide dissociated within 2 h. In contrast, when Aβ was deposited over longer load times (within the second linear phase of Figure 1), nearly all of the deposited Aβ remained bound to the template for the duration of the dissociation experiment (at least 3 days). Further, the percentage of deposited Aβ remaining essentially irreversibly bound to the template increased with deposition load time, suggesting that irreversible amyloid accumulation is directly related to the duration of time the depositing peptide interacts with the amyloid template.

The dissociation time course measured at each of the load times closely ($r^2 > 0.99$) fits a double-exponential dissociation equation

$$Y = (A)e^{(-k_1)t} + (1 - A)e^{(-k_2)t} + C$$

where Y is the fraction of Aβ remaining bound to the template, A is the fractional contribution and $-k_1$ is the dissociation rate constant of the first process, t is the dissociation time, $(1 - A)$ is the fractional contribution, and $-k_2$ is the dissociation rate constant of the second process, and C is a

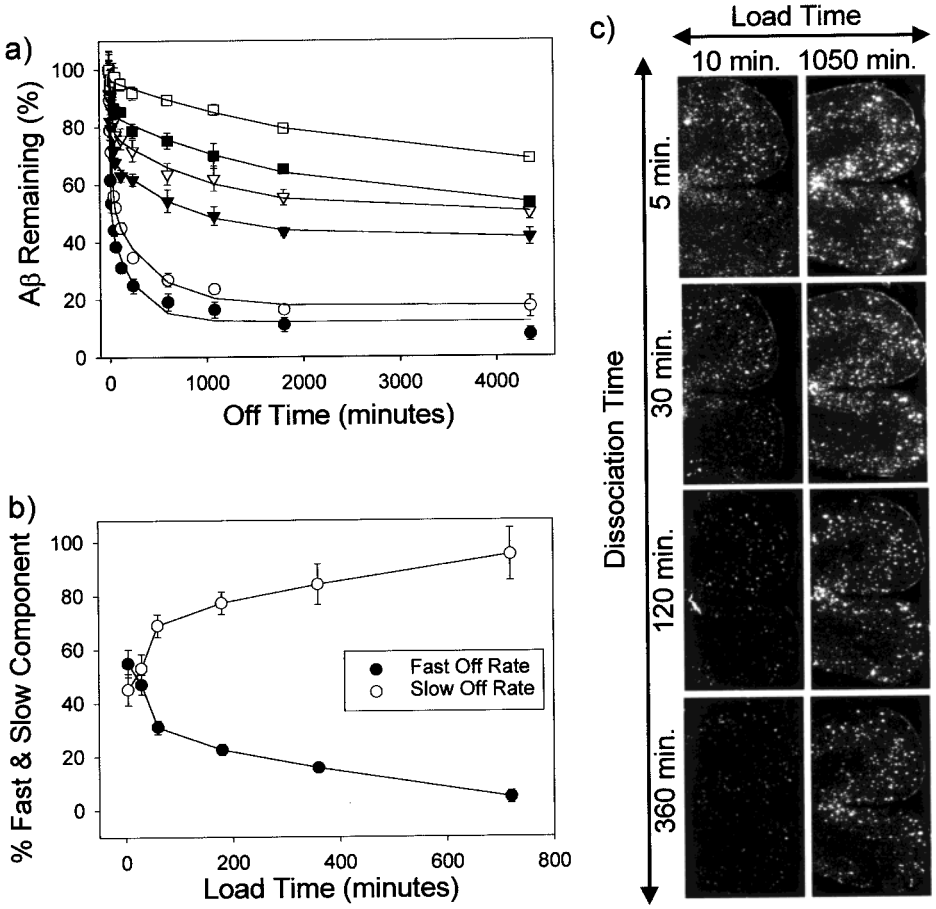

FIGURE 2: Dissociation of deposited Aβ. (a) Dissociation time course of deposited Aβ. [^{125}I]Aβ was deposited onto synthetic amyloid fibrils immobilized in 96 well plates for load times of 5 min (●), 30 min (○), 60 min (▼), 180 min (▽), 360 min (■), and 720 min (□). Following the deposition incubation (load), the dissociation of deposited radiolabeled Aβ was measured for each load time by soaking the immobilized fibrils with buffer. Values are reported as the percent of deposited [^{125}I]Aβ remaining vs dissociation time. Error bars represent the standard deviation of 5 measurements. (b) Relative contributions of a fast and a slow dissociation rate component to Aβ dissociation time course. The dissociation time course data for each load time in panel a were fit to the double exponential equation $Y = (A)e^{(-k_1)t} + (1 - A)e^{(-k_2)t} + C$. The relative contribution of the fast (reversible) dissociation rate component $(A)e^{(-k_1)t}$ and the slow (irreversible) dissociation rate component $(1 - A)e^{(-k_2)t} + C$ to each dissociation time course was plotted vs the load (deposition) time. Error bars represent the uncertainty in the regression measurements of the equation components. (c) Dissociation of [^{125}I]Aβ deposited onto brain amyloid was measured for load times of 10 or 1050 min. Following the removal of the radiolabeled Aβ solution the dissociation of the deposited Aβ was determined for 5, 30, 120, and 360 min off times. Images shown are dark-field autoradiograms, where light areas represent the sites and intensities of radiolabeled Aβ deposition. Different film exposure times were used for the short (10 min) and long (1050 min) load time experiments so the images would be of comparable intensity at the 5 min dissociation time.

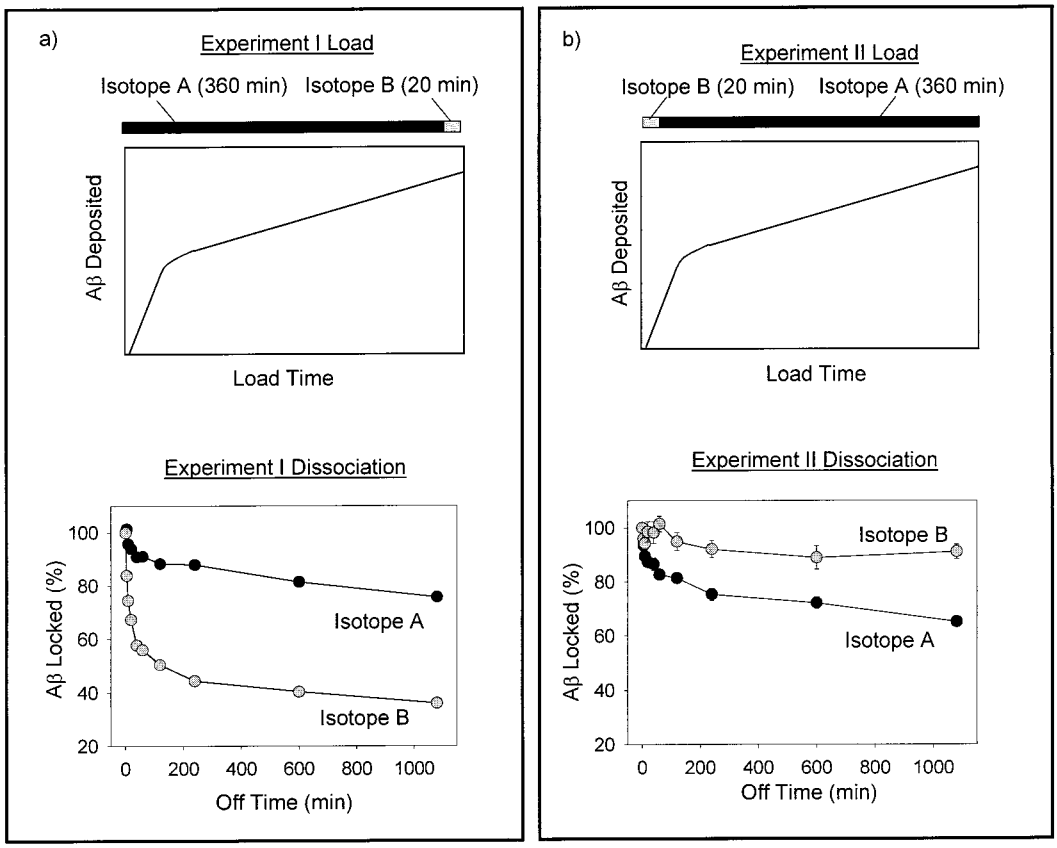

FIGURE 3: Aβ deposited first dissociates last. A double-label pulse-chase experiment was performed using [^{125}I]Aβ and [^{131}I]Aβ to determine the temporal order of the dissociation of Aβ deposited in the initial dock phase and the subsequent lock phase. (a) In the first experiment, a pulse of Aβ-isotope A was incubated with the template for 6 h. Following this first incubation, the template was rapidly rinsed and then incubated (chased) with Aβ-isotope B for 20 min. Following the second Aβ incubation, the dissociation time courses of the Aβ-isotope A and Aβ-isotope B were measured. (b) In the second experiment, a pulse of Aβ-isotope B was incubated with the template for 20 min. Following this first incubation, the template was rapidly rinsed and the template was incubated (chased) with Aβ-isotope A for 6 h. Following the second Aβ incubation, the dissociation time courses of the Aβ-isotope B and the Aβ-isotope A were measured. Importantly, on a molar basis, the amount of Aβ bound to the template during the short load was similar whether this load preceded or followed the 6 h load. Results were indistinguishable whether ^{125}I and ^{131}I were used for isotope A and isotope B, respectively, or isotope B and isotope A, respectively. The results of this experiment establish that Aβ deposited during the reversible "dock" phase of deposition latter becomes irreversibly "locked" onto the template.

constant. The first (faster) dissociation process had a half time of 10.4 $\pm$ 2.1 min, while the half time for the second (slower) dissociation process was at least 100-fold longer. A constant, *C*, which represents the fraction of the material that does not dissociate from the template on a time scale of several days, was required for optimal fit.

While the rate constants k_1 and k_2 did not appear to vary as a function of load time, the fractional coefficients for the two dissociation processes were strongly related to the time the depositing peptide was exposed to the template. With increased deposition load time, the contribution of the slow dissociation process increased while the contribution of the fast dissociation process correspondingly decreased (Figure 2b). Consistent with these observations, for the shortest load times, the dissociation time course could be described by a single-exponential decay with a rate constant similar to that of the fast dissociation component (k_1). Likewise for the longest load times, the dissociation time course could be described with a single-exponential decay equation with a rate constant similar to that of the slow dissociation component (k_2). For intermediate load times, a single-exponential decay equation fit the data poorly.

We also examined the dissociation properties of radiolabeled Aβ deposited onto authentic brain amyloid in unfixed sections of human AD cortex (Figure 2c). As was observed for deposition onto synthetic amyloid fibrils, the fraction of radiolabeled Aβ deposited onto brain amyloid in human brain ex vivo, which remains irreversibly bound was strongly dependent on the load time. When the labeled peptide was exposed to the tissue amyloid for a short (10 min) load time, very little ($\approx$10%) of the deposited peptide remained bound to the amyloid after 6 h. In contrast, when the labeled peptide was exposed to the tissue amyloid for a long (1050 min) load time, most ($\approx$70%) of the deposited peptide remained bound to the amyloid after 6 h. These results establish that the dissociation of Aβ deposited onto authentic AD brain amyloid, like Aβ deposited onto the synthetic amyloid template, is highly dependent on the time the peptide interacted with the template.

To further examine the mechanism of Aβ deposition, we employed a double label pulse-chase experiment to determine if the fast and slow dissociation rate processes were a consequence of Aβ interaction with a common site or distinct types of sites on the template. We utilized [^{125}I]Aβ and [^{131}I]Aβ, which can be unambiguously distinguished by γ-emission energies, to allow determination of the temporal sequence of dissociation for alterations in pulse and chase time length for exposure to a template of synthetic amyloid

(Figure 3). Following a pulse of one radiolabeled Aβ isotope and a chase with the second radiolabeled Aβ isotope, dissociation times for the two isotopes were measured. When a long pulse of "Aβ-isotope A" preceded a short chase of the "Aβ-isotope B", approximately 80% of the Aβ-isotope A deposited onto the template over the long pulse remained bound to the template (Figure 3a). However, nearly all of the Aβ-isotope B deposited during the short chase rapidly dissociated from the template (Figure 3a). In contrast, when the short pulse of Aβ-isotope B preceded the long chase with Aβ-isotope A (Figure 3b), essentially all of the Aβ-isotope B deposited in the short pulse remained bound to the template. These results demonstrate that while Aβ deposited onto the template during a short load time is reversibly bound to the template, the Aβ deposited during this short time later becomes irreversibly incorporated into the template in a time-dependent manner.

To further probe the relevance of our model of Aβ amyloid propagation to human disease, we examined the deposition kinetics of Aβ peptides bearing sequence alterations implicated in increased risk for Aβ amyloidosis. A long form of Aβ, Aβ(1−42), and an Aβ peptide with the single amino acid substitution E22Q is strongly implicated in human Aβ amyloidoses (*4*, *25*, *26*). When all three peptides were examined under identical conditions, both Aβ(1−42) and Aβ(1−40)-E22Q showed two-phase kinetics (not shown) with an enhanced rate of locking relative to Aβ(1−40). A substantially lower fraction of deposited Aβ(1−42) and Aβ-(1−40)-E22Q relative to the wild-type Aβ(1−40) peptide dissociated at load times ranging from 30 min (Figure 4a) to 720 min (Figure 4b). When the molar amounts of deposited peptide "locked" onto the template vs load times were compared (Figure 4c), Aβ(1−40)-E22Q displayed the greatest amount of Aβ congener locked with approximately 3-fold more deposited peptide locked than was observed for Aβ(1−40). Similarly, Aβ(1−42) displayed substantially (about 2-fold) more deposited peptide locked relative to Aβ-(1−40). The rank order of the peptides Aβ(1−40)-E22Q > Aβ(1−42) > Aβ(1−40) in their "lock" kinetics is consistent with their overall amyloidogenicities expected from the age of symptom onset in patients that produce these altered forms of Aβ (*4*).

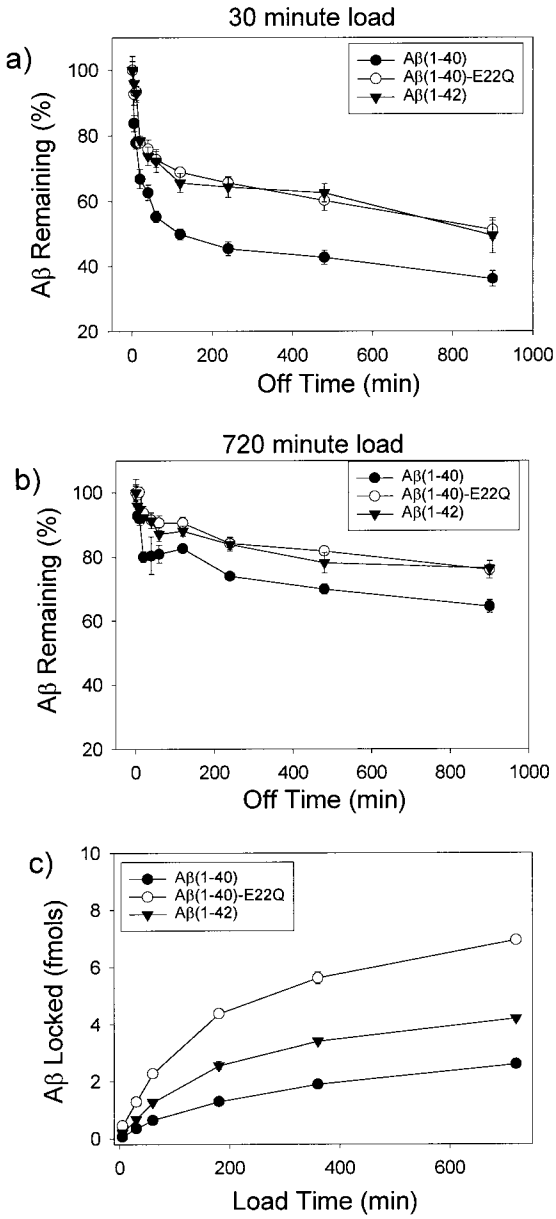

FIGURE 4: Dissociation time courses of Aβ(1−40), Aβ(1−40)-E22Q, and Aβ(1−42). (a) Radiolabeled Aβ(1−40), Aβ(1−40)-E22Q, and Aβ(1−42) at identical concentrations were deposited in parallel onto immobilized Aβ(1−40) fibrils for 30 min. Following this incubation, the dissociation of the deposited peptides was measured as described. (b) Dissociation time courses were also measured following a 720 min load. (c) The amount of Aβ(1−40), Aβ(1−40)-E22Q, and Aβ(1−42) "locked" (fmols remaining after 900 min of dissociation time) was quantified for each of several load times ranging from 5 to 720 min.

DISCUSSION

The kinetic data presented here support a model of amyloid growth in which the depositing monomeric (*7*, *32*) peptide initially interacts with the Aβ fibril template in a reversible manner. However, exposure to and interaction with the template leads to a time-dependent transition in which the Aβ molecules deposited earlier become irreversibly associated with the template by a distinct process. This observation has several significant implications for understanding the dynamics and mechanism of amyloid accumulation in AD and inhibiting the process as a means of therapeutic intervention (vide infra). Cruz et al. (*27*) have proposed a model of amyloid plaque formation where Aβ assembly and disassembly are critical factors in the dynamics of plaque maturation. While our results establish the reversibility of early interaction between the depositing peptide and the template, a time-dependent transition to irreversible association, most likely a critical factor in disease progression, is also evident. The data presented here are thus consistent with the presence of reversible and irreversible interactions in amyloid and provide a mechanistic context in which such interactions contribute to fibril growth in AD.

The results presented here establish that at physiological concentrations (picomolar to nanomolar) and conditions (PBS), at least in vitro, the most recently deposited Aβ peptide is susceptible to dissociation, while molecules deposited earlier are essentially irreversibly incorporated into the growing fibril. Multiphase deposition kinetics have also been reported (*33*) at much higher Aβ concentrations, using surface plasmon resonance. Although agents that simply lower the concentration of soluble Aβ would be expected to

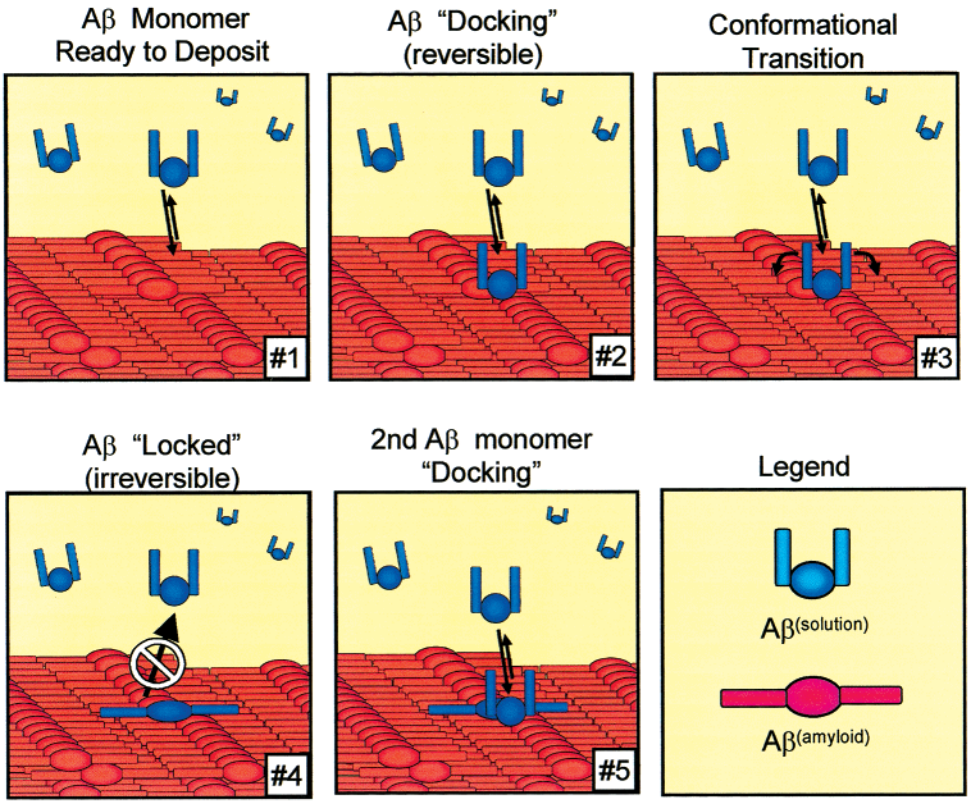

FIGURE 5: Schematic model of Aβ deposition. The data presented here indicate that the process of Aβ deposition is mediated by at least two steps. In the first step "dock" (1 to 2), depositing Aβ interacts with the amyloid template in a reversible manner. In the second step "lock" (3 to 4), the "docked" Aβ undergoes a time dependent transition to irreversible interaction with the template. Finally, it is likely that the "locked" Aβ can serve as a template for deposition of a subsequent Aβ monomer (5). Since Aβ deposition requires a conformational transition in the depositing peptide, time-dependent conversion of $A\beta^{(docked)}$ to $A\beta^{(locked)}$ is most likely a kinetic observation of template mediated conformational rearrangement.

inhibit further amyloid deposition, the chemical stability of "locked" Aβ suggests that they would be significantly less effective at reducing existing amyloid burden. Consequently, it is almost certain that the reduction of Aβ amyloid burden following immunization of aged transgenic animals against Aβ (*28*) is a consequence of a direct biological action on the fibrillar amyloid rather than an indirect consequence of an action on monomeric Aβ in solution. These observations suggest that biological or chemical treatments that increased microglial phagocytosis or other biological clearance of fibrils, rather than simply increasing the clearance or decreasing the production of monomeric Aβ, would be a more successful strategy to reduce existing amyloid burden present prior to treatment.

A key prediction of our two-phase kinetic model (Figure 5) of Aβ deposition is a break point in the time course between the slope of the first linear phase and the second linear phase, indicative of a rate-limiting slow step in the steady-state process. It is likely that this break point is a consequence of the buildup of docked Aβ, which would not be expected to serve as a template for further Aβ deposition, while Aβ that has locked may serve as a self-complementary template for deposition of additional Aβ. Consequently, once the steady-state between $A\beta^{(solution)}$ and $A\beta^{(docked)}$ has been reached, the overall rate of Aβ deposition is limited by the relatively slow conversion of $A\beta^{(docked)}$ to $A\beta^{(locked)}$.

While a conformational transition from the partially folded monomer to β-sheet is almost surely an essential component in the conversion of $A\beta^{(solution)}$ to $A\beta^{(amyloid)}$ (*1*−*3*, *12*), it is critical to establish the molecular context in which such a rearrangement occurs. The most parsimonious interpretation of the present observations is that interaction with preexisting amyloid guides and facilitates conversion of $A\beta^{(solution)}$ to $A\beta^{(amyloid)}$. Our data support a steady-state model (Figure 5) of Aβ amyloid growth in which at least two processes are essential. The initial step of this mechanism is a reversible pseudo-equilibrium between $A\beta^{(solution)}$ and $A\beta^{(docked)}$. Once this dynamic is established, the slower rate-limiting step, conversion of $A\beta^{(docked)}$ to $A\beta^{(transition\ state)}$, accounts for the "kinetic trap" and the reduction in the slope of Aβ deposition time course at later time points. A likely means by which this may occur is an induced fit mechanism, in which the growing fibril serves as a template to lower the activation energy of the conversion of $A\beta^{(solution)}$ to $A\beta^{(transition\ state)}$ in a manner similar to the way an enzyme or other catalyst directs the positioning of a substrate to facilitate a chemical reaction. Once $A\beta^{(docked)}$ has been converted to $A\beta^{(transition\ state)}$, conversion to $A\beta^{(locked)}$ would occur relatively quickly. Thus, it is likely that the time-dependent conversion of $A\beta^{(docked)}$ to $A\beta^{(locked)}$ is a kinetic observation of the rate-limiting step in the conformational transition of $A\beta^{(solution)}$ to $A\beta^{(amyloid)}$. After conversion to $A\beta^{(amyloid)}$, the deposited peptide, newly locked, could serve as a self-complementary template for deposition of an additional Aβ monomer, consistent with observed nonsaturability (*2*, *16*). Template mediated conformational transitions have also been hypothesized to contribute to the conversion of PrP^{C} to PrP^{Sc} in the prion diseases (*21*) and to the assembly of viral coat proteins (*29*). Thus, several forms

of normal and abnormal protein assembly may share this mechanism.

While the present results indicate that preexisting amyloid can serve as a specific template to guide the transition from $A\beta^{(soluble)}$ to $A\beta^{(amyloid)}$ during amyloid growth, an important factor in the initiation of AD would be the early events that lead to de novo $A\beta^{(amyloid)}$ formation. Lansbury and coworkers have proposed that at high concentrations (10^{-4} M), synthetic Aβ spontaneously nucleates to form "seeds" which later propagate to fibrils that grow by a nucleation independent mechanism (*30*). However, the kinetics of Aβ nucleation suggest that formation of a "seed" would take at least thousands of years to occur spontaneously at physiological (10^{-9} M) Aβ concentrations.

As Aβ fibrils can serve as a template to transform $A\beta^{(solution)}$ to $A\beta^{(amyloid)}$ at physiological concentrations, it is possible that other proteins can serve as a "molecular scaffold" to guide the conversion of the semi-folded $A\beta^{(solution)}$ monomer to an amyloid-like conformation which could subsequently serve as a new template for Aβ assembly. Thus, facilitated conformational rearrangement and subsequent Aβ assembly is a potential mechanism by which the first steps in Aβ amyloid formation may occur independent of unfacilitated nucleation. Consistent with this hypothesis, a component in conditioned cell media is competent to promote Aβ assembly at physiological Aβ concentrations under conditions where spontaneous Aβ nucleation does not occur (*31*). Further, some proteins with substantial β-sheet content also serve as heterologous templates for Aβ assembly in vitro by a nucleation-independent mechanism (not shown). Cohen and Prusiner have proposed that an unidentified protein termed "protein X" serves as a facilitator for the conversion of PrP^{C} to PrP^{Sc} in prion disorders (*21*). We suggest that the mechanism of template-mediated conformational rearrangement guided by homologous or heterologous proteins is shared in Alzheimer's disease and the prion diseases, among other protein assembly processes.

The nonequilibrium kinetics and the thermodynamics of Aβ amyloid assembly have suggested that only extremely high-affinity inhibitors could slow the process. The present study, however, demonstrates that AD has a kinetic vulnerability and illuminates an attractive target for therapeutic intervention. [Other protein assembly disorders very likely share with AD a kinetic vulnerability.] While Aβ is essentially irreversibly incorporated into the growing fibril in the "lock" phase of deposition, an initial reversible weak "docking" interaction is required to enable subsequent "locking" interactions between the template and the depositing peptide. Consequently, the affinity of a pharmacophore for the amyloid template would need only be sufficient to inhibit reversible low-affinity Aβ docking to inhibit the subsequent irreversible lock phase of deposition and thus block the transition from $A\beta^{(solution)}$ to $A\beta^{(amyloid)}$.

ACKNOWLEDGMENT

We thank E. T. Wallick for helpful discussions and J. R. Marshall and G. F. Egnaczyk for critical reading of the manuscript.

REFERENCES

1. Kelly, J. W. (1998) *Curr. Opin. Struct. Biol. 8*, 101−6.
2. Maggio, J. E., and Mantyh, P. W. (1996) *Brain Pathol. 6*, 147−62.
3. Wetzel, R. (1996) *Cell 86*, 699−702.
4. Selkoe, D. J. (1997) *Science 275*, 630−1.
5. Selkoe, D. J. (1994) *J. Neuropathol. Exp. Neurol. 53*, 438−47.
6. Lee, J. P., Stimson, E. R., Ghilardi, J. R., Mantyh, P. W., Lu, Y. A., Felix, A. M., Llanos, W., Behbin, A., Cummings, M., and Van Criekinge, M., et al. (1995) *Biochemistry 34*, 5191−200.
7. Lee, J. P., Clish, C. B., Hassell, D. R., Mehr, K. G., Barbara, T. M., and Maggio, J. E. (1999) *Amyloid* (submitted for publication).
8. Lee, J. P., Stimson, E. R., Zhang, S. S., Lu, Y. A., Felix, A. M., and Maggio, J. E. (1999) *J. Struct. Biol.* (submitted for publication).
9. Kirschner, D. A., Abraham, C., and Selkoe, D. J. (1986) *Proc. Natl. Acad. Sci. U.S.A. 83*, 503−7.
10. Lansbury, P. T., Jr., Costa, P. R., Griffiths, J. M., Simon, E. J., Auger, M., Halverson, K. J., Kocisko, D. A., Hendsch, Z. S., Ashburn, T. T., and Spencer, R. G., et al. (1995) *Nat. Struct. Biol. 2*, 990−8.
11. Halverson, K., Fraser, P. E., Kirschner, D. A., and Lansbury, P. T., Jr. (1990) *Biochemistry 29*, 2639−44.
12. Esler, W. P., Felix, A. M., Stimson, E. R., Ghilardi, J. R., Lu, Y.-A., Vinters, H. V., Mantyh, P. W., Lee, J. P., and Maggio, J. E. (2000) *J. Struct. Biol.* (in press).
13. Lomakin, A., Teplow, D. B., Kirschner, D. A., and Benedek, G. B. (1997) *Proc. Natl. Acad. Sci. U.S.A. 94*, 7942−7.
14. Kusumoto, Y., Lomakin, A., Teplow, D. B., and Benedek, G. B. (1998) *Proc. Natl. Acad. Sci. U.S.A. 95*, 12277−82.
15. Mantyh, P. W., Stimson, E. R., Ghilardi, J. R., Allen, C. J., Dahl, C. E., Whitcomb, D. C., Vigna, S. R., Vinters, H. V., Labenski, M. E., and Maggio, J. E. (1991) *Bull. Clin. Neurosci. 56*, 73−85.
16. Maggio, J. E., Stimson, E. R., Ghilardi, J. R., Allen, C. J., Dahl, C. E., Whitcomb, D. C., Vigna, S. R., Vinters, H. V., Labenski, M. E., and Mantyh, P. W. (1992) *Proc. Natl. Acad. Sci. U.S.A. 89*, 5462−6.
17. Esler, W. P., Stimson, E. R., Ghilardi, J. R., Vinters, H. V., Lee, J. P., Mantyh, P. W., and Maggio, J. E. (1996) *Biochemistry 35*, 749−57.
18. Jarrett, J. T., and Lansbury, P. T., Jr. (1992) *Biochemistry 31*, 12345−52.
19. Lomakin, A., Chung, D. S., Benedek, G. B., Kirschner, D. A., and Teplow, D. B. (1996) *Proc. Natl. Acad. Sci. U.S.A. 93*, 1125−9.
20. Naiki, H., and Nakakuki, K. (1996) *Lab. Invest. 74*, 374−83.
21. Cohen, F. E., and Prusiner, S. B. (1998) *Annu. Rev. Biochem. 67*, 793−819.
22. Esler, W. P., Stimson, E. R., Ghilardi, J. R., Lu, Y. A., Felix, A. M., Vinters, H. V., Mantyh, P. W., Lee, J. P., and Maggio, J. E. (1996) *Biochemistry 35*, 13914−21.
23. Esler, W. P., Stimson, E. R., Ghilardi, J. R., Felix, A. M., Lu, Y. A., Vinters, H. V., Mantyh, P. W., and Maggio, J. E. (1997) *Nat. Biotechnol. 15*, 258−63.
24. Esler, W. P., Stimson, E. R., Mantyh, P. W., and Maggio, J. E. (1999). In *Methods in Enzymology Amyloid, Prions, and Other Protein Aggregates* (Wetzel, R., Ed.) Volume 309, pp 350−374, Academic Press, San Diego, CA.
25. Scheuner, D., Eckman, C., Jensen, M., Song, X., Citron, M., Suzuki, N., Bird, T. D., Hardy, J., Hutton, M., Kukull, W., Larson, E., Levy-Lahad, E., Viitanen, M., Peskind, E., Poorkaj, P., Schellenberg, G., Tanzi, R., Wasco, W., Lannfelt, L., Selkoe, D., and Younkin, S. (1996) *Nat. Med. 2*, 864−70.
26. Levy, E., Carman, M. D., Fernandez-Madrid, I. J., Power, M. D., Lieberburg, I., van Duinen, S. G., Bots, G. T., Luyendijk, W., and Frangione, B. (1990) *Science 248*, 1124−6.
27. Cruz, L., Urbanc, B., Buldyrev, S. V., Christie, R., Gomez-Isla, T., Havlin, S., McNamara, M., Stanley, H. E., and Hyman, B. T. (1997) *Proc. Natl. Acad. Sci. U.S.A. 94*, 7612−6.
28. Schenk, D., Barbour, R., Dunn, W., Gordon, G., Grajeda, H., Guido, T., Hu, K., Huang, J., Johnson-Wood, K., Khan, K., Kholodenko, D., Lee, M., Liao, Z., Lieberburg, I., Motter, R.,

Mutter, L., Soriano, F., Shopp, G., Vasquez, N., Vandevert, C., Walker, S., Wogulis, M., Yednock, T., Games, D., and Seubert, P. (1999) *Nature 400*, 173−7.
29. Galisteo, M. L., Gordon, C. L., and King, J. (1995) *J. Biol. Chem. 270*, 16595−601.
30. Jarrett, J. T., and Lansbury, P. T., Jr. (1993) *Cell 73*, 1055−8.
31. Podlisny, M. B., Walsh, D. M., Amarante, P., Ostaszewski, B. L., Stimson, E. R., Maggio, J. E., Teplow, D. B., and Selkoe, D. J. (1998) *Biochemistry 37*, 3602−11.
32. Tseng, B. P., Esler, W. P., Stimson, E. R., Ghilardi, J. R., Vinters, H. V., Mantyh, P. W., and Maggio, J. E. (1999) *Biochemistry 38*, 10242−31.
33. Myszka, D. G., Wood, S. J., and Biere, A.-L. (1999). In *Methods in Enzymology Amyloid, Prions, and Other Protein Aggregates* (Wetzel, R., Ed.) Volume 309, pp 386-402, Academic Press, San Diego, CA.

BI992933H